



## Preparation of the activated carbon from India shrub wood and their application for methylene blue removal: modeling and optimization

M. Pirsaeheb<sup>a,\*</sup>, Z. Rezaei<sup>b</sup>, A.M. Mansouri<sup>a,c,\*</sup>, A. Rastegar<sup>d</sup>, A. Alahabadi<sup>d</sup>,  
A. Rahmani Sani<sup>d</sup>, K. Sharafi<sup>e</sup>

<sup>a</sup>Research Center for Environmental Determination of Health (RCEDH), Kermanshah University of Medical Science, Kermanshah, Iran, Tel. +98 9123446880; Fax: +98 8314274559; email: [mpirsaeheb@yahoo.com](mailto:mpirsaeheb@yahoo.com) (M. Pirsaeheb), Tel. +98 9183431787; emails: [ammansouri34@yahoo.com](mailto:ammansouri34@yahoo.com), [yadollamansouri@yahoo.com](mailto:yadollamansouri@yahoo.com) (A.M. Mansouri)

<sup>b</sup>Student Research Committee, Kermanshah University of Medical Science, Kermanshah, Iran, Tel. +98 930516713; email: [rezaiz41@yahoo.com](mailto:rezaiz41@yahoo.com)

<sup>c</sup>Faculty of Chemistry, Department of Analytical Chemistry, Razi University, Kermanshah, Iran

<sup>d</sup>Department of Environmental Health Engineering, School of Public Health, Sabzevar University of Medical Sciences, Sabzevar, Iran, Tel. +98 9159833229; email: [rastegar.89@gmail.com](mailto:rastegar.89@gmail.com) (A. Rastegar), Tel. +98 9151713424; email: [ahmad\\_health@yahoo.com](mailto:ahmad_health@yahoo.com) (A. Alahabadi), Tel. +98 9151708204; email: [rahmani240@gmail.com](mailto:rahmani240@gmail.com) (A.R. Sani)

<sup>e</sup>Department of Environmental Health Engineering, School of Public Health, Kermanshah University of Medical Sciences, Kermanshah, Iran, Tel. +98 9183786; email: [kio.sharafi@gmail.com](mailto:kio.sharafi@gmail.com)

Received 6 August 2014; Accepted 27 December 2014

---

### ABSTRACT

In this article, we investigated the use of activated carbon (AC) obtained from India shrub wood for the removal of methylene blue (MB) from aqueous solutions. The properties of this adsorbent, such as BET surface area, pore volume and pores diameter, were characterized from N<sub>2</sub> adsorption isotherms. It was found that the prepared AC is essentially mesoporous, and that the BET surface area was 1,024 m<sup>2</sup>/g. The experimental design was conducted based on a central composite design and the data were analyzed using response surface methodology. The biosorption process was investigated as a function of three independent factors viz. contact time, initial solution pH (2–10), and adsorbent dosage (0.2–1 g/L). Equilibrium isotherms were analyzed with Langmuir, Freundlich, and Dubinin–Radushkevich isotherm equations using correlation coefficients. Adsorption data were well described by the Langmuir model, although they could be modeled by the Freundlich as well. The maximum MB adsorption capacity of prepared AC was 257.73 mg/g. In order to test the experimental data, different kinetic models were applied. It was concluded that the pseudo-second-order kinetic model provided better correlation of the experimental data than other models. Thermodynamic parameters ( $\Delta H^\circ$ ,  $\Delta G^\circ$ , and  $\Delta S^\circ$ ) were determined and the adsorption process was found to be at the state between physical and chemical sorption, spontaneous, and an endothermic one.

*Keywords:* Adsorption; Isotherm; Activated carbon; Dye removal; Chemical kinetic; India shrub wood

---

\*Corresponding authors.

## 1. Introduction

One of the main pollutants generated from chemical industries, such as textile leather, paper, and dye manufacturing industries, is dye. According to the literature, there are over 100,000 commercially available dyes with a production of over  $7 \times 10^5$  metric tons per year [1]. The wide application of dyes generates colored wastewaters, which are extremely noxious to the aquatic biota and upset the natural balance in the water resources through reduced photosynthetic activity. Some adverse impacts of dyes on humans (allergy, dermatitis, skin irritation, and cancer) are also reported in the literature [2]. The color is the first contaminant to be recognized in wastewater, and the presence of even very small amount of dyes in water—less than 1 ppm for some dyes—is highly visible and undesirable [3,4]. Therefore, it is very important to treat the colored synthetic compounds because they are hazardous to human being and environments.

There has recently been an increase in research activity focusing on treating colored wastewaters; numerous techniques have also been proposed for the removal of dyes from wastewater samples. Several techniques are reported in this regard, such as the use of adsorption, coagulation, flocculation, oxidation, precipitation, filtration, electrochemical processes, etc. [5]. However, chemical methods of dye removal produce a large amount of sludge, which can cause disposal problems [6,7]. Furthermore, these methods need chemicals and electrical energy, which further pose problems for the environment [8,9].

Amongst the techniques, adsorption seems to be one of the economical and most effective methods because of its simple operation and easy handling. The high cost of the removal of dyes from aqueous solutions using adsorption on commercial activated carbons, though very effective, has motivated the search for alternative adsorbents. In recent years, researchers have studied the production of activated carbon (AC) from cheap and renewable precursors, such as olive husk [10], jute fiber [11], biomass fly ash [12], coffee endocarp [13], cotton stalks [14], plum kernels [15], groundnut shells and *Eichhornia* [16], palm kernel fiber [17], bamboo [18], modified peanut husk [19], and modified *Eichhornia* charcoal [20,21].

Methylene blue (MB) is a cationic dye that is most commonly used for coloring. It is generally used for dyeing cotton, wool, and silk. This dye has been studied because of its known strong adsorption into solids, and it often serves as a model compound for the removal of organic contaminants and colored bodies from aqueous solutions [22].

In the last few years, the response surface methodology (RSM) has been applied to optimize and evaluate interactive effects of independent factors in numerous chemical and biochemical processes. The RSM is a statistical technique for designing experiments, building models, evaluating the effects of several factors, and searching optimum conditions for desirable responses and reducing the number of experiments [23–25].

In this study, India shrub wood, which is a renewable, abundant, and cheap plant-based material was used as an AC source due to lack of information on its adsorption abilities for dye adsorption. The effect of various parameters, such as contact time, solution pH, and adsorbent dosage on the adsorption of MB onto this sorbent was also systematically studied. Likewise, adsorption isotherms, kinetic, and thermodynamic were evaluated. Furthermore, in order to evaluate the interactions between the variables as well as their direct impacts on the process, the central composite design (CCD) has been applied to the analysis and optimization of adsorptive removal of MB from aqueous solutions.

## 2. Materials and methods

### 2.1. Materials

The basic dye used in this study was MB purchased from Sigma-Aldrich. MB has molecular formula  $C_{16}H_{18}N_3ClS$  (Mol. wt. 319.85 g/mol). The maximum wavelength of this dye is 664 nm. The pH of the solutions was adjusted to the required value (range: 2–10) by adding either 1 M HCl or 1 M NaOH solution. Aluminum chloride was supplied from Merk.

### 2.2. Preparation of AC from India shrub wood

India shrub wood used in this study was collected from the deserts around Mashhad, Iran. The precursor was air-dried, crushed, and sieved to obtain a geometrical mean size ranging from 1.0 to 5 cm. Subsequently, it was loaded on a stainless steel boat and carbonized at 550°C for 1 h under nitrogen atmosphere (at the heating rate of 10°C/min) inside a horizontal furnace. After this stage, the amount of 10 g produced carbon was mixed with ammonium chloride (0.2 g) and 100 mL of water, at the inner of a vertical stainless steel reactor under magnetic stirring for 2 h, and then it was dried at 105°C for 1 h. After cooling, the resulting mixture was washed with a 0.1 M

solution of HCl followed by hot distilled water until pH ~6.4 to eliminate activating agent residues, and other inorganic species formed during the process. The obtained carbon was dried at 800°C for 2 h and kept in tightly closed bottles for further analysis. The characteristics of produced AC are shown in Table 1.

### 2.3. Analytical methods

A surface morphology of produced AC was studied by scanning electron microscopy using a Philips XL30 microscope at an accelerating voltage of 10 kV. A Fourier transformed infrared (FTIR) was carried out using a spectrometer (ABB BOMEM MB 104 SERIES, SWIS) in the transmittance mode at 50 scans with a resolution of 4 cm<sup>-1</sup> in the range of 800–4,000 cm<sup>-1</sup> with KBr pellets technique. N<sub>2</sub> adsorption/desorption isotherms (BET) at 77 K were measured on BELSORP-mini II (Bel, Japan). To determine dye in the solution samples, the mixture was allowed to settle, and then was centrifuged at 2,000 rpm for 15 min. The concentrations of dye were measured with a UV–visible spectrophotometer (Hitachi Model 100-40) at the appropriate wavelength corresponding to the maximum absorbance of MB, 664 nm.

### 2.4. Adsorption experiment

Adsorption experiments were carried out in 500 mL Erlenmeyer flasks by using five different concentrations of MB at a temperature of 28 ± 2°C. A certain amount of AC was mixed with 250 mL MB solutions of concentrations ranging from 50 to 300 mg/L. The amount of MB adsorbed on the AC was calculated from the difference between the initial concentration of the MB and the residual MB concentration in the solution. The calculation can be described by the following equation:

$$q_e = \frac{(C_0 - C_e)V}{M} \quad (1)$$

where  $q_e$  (mg/g) is the adsorbent capacity,  $C_0$  (mg/L) is the initial concentration of MB,  $C_e$  (mg/L) is the

final or the equilibrium concentration of MB,  $V$  is the experimental solution volume (L), and  $M$  is the weight of AC powder (g).

### 2.5. Experimental design

RSM along with the design of experiments remove systematic errors with an estimate of the experimental errors, and also reduce the number of experiments, in order to obtain the optimum operating conditions. There are many classes of response surface designs that are occasionally useful in practice, such as CCD, Box-Behnken design, hybrid design, and three-level factorial design [26]. Among these methods, the CCD is the most frequently used one under RSM. The RSM employed in the current study was CCD involving three different factors, that is, contact time ( $A$ ), adsorbent dosage ( $B$ ), and pH ( $C$ ). The investigated range for these variables is presented in Table 2.

The adsorption capacity of the prepared AC powder was evaluated based on the CCD experimental plan (Table 3). The design consisted of  $2k$  factorial points augmented by  $2k$  axial points and a center point, where  $k$  is the number of variables. The coded values of three operating variables ( $A$ ,  $B$ , and  $C$ ) were set at five levels: -1.5 (minimum), -1, 0 (central), +1, and +1.5 (maximum). These five levels were assessed based on the full face-centered CCD experimental plan.

Accordingly, 20 experiments ( $=2^k + 2k + 6$ ), where  $k$  is the number of factors, were conducted with 15 experiments organized in a factorial design (including eight factorial points, six axial points, and one center point), and the remaining five involving the replication of the central point, in order to get a good estimate of the experimental errors. Repetition experiments were carried out, which were followed by the order of runs designed by DOE as shown in Table 3.

Table 1

Characteristic of produced activated carbon from India shrub wood

BET (m <sup>2</sup> /g)	1,024
pH <sub>pzc</sub>	6.5
Pores structure	Mesopore
Total pore volume (P/P0 = 0.990)	0.572

Table 2

Experimental range and levels of the independent variables

Variables	Range and levels				
	-α (-1.5)	-1	0	1	+α (1.5)
Contact time (min)	5	25	45	65	85
Adsorbent dosage (g/L)	0.2	0.4	0.6	0.8	1
pH	2	4	6	8	10

Table 3  
Experimental conditions and results of CCD

Run	Variables			Responses			
	Factor 1	Factor 2	Factor 3	MB removal (%)	q (mg/g)		
	A: Contact time (min)	B: Adsorbent dosage (mg/L)	C: pH		Actual (%)	Actual (mg/g)	Predicted (mg/g)
1	45	0.6	6	10	89.11	231.85	231.65
2	5	1	10	6	95.06	145.06	145.19
3	45	0.8	6	10	99.43	186.76	165.86
4	85	1	10	6	99.58	149.58	152.29
5	45	0.6	6	2	88.91	226.52	231.65
6	5	0.2	2	2	18.66	343.3	347.98
7	85	1	2	6	99.01	149.01	147.75
8	45	0.6	6	10	89.23	235.38	0.13
9	85	0.2	10	6	43.61	468.05	471.33
10	65	0.6	6	6	91.64	236.07	241.88
11	45	0.6	6	8	89.41	230.68	0.11
12	45	0.6	8	6	98.2	247	249.90
13	45	0.6	6	10	88.91	231.52	0.11
14	5	0.2	10	4	30.69	403.45	396.60
15	45	0.6	4	2	90.24	233.73	236.61
16	85	0.2	2	6	36.19	430.95	422.71
17	45	0.4	6	6	67.09	292.73	297.45
18	25	0.6	6	2	86.08	226.8	221.43
19	5	1	2	6	86.53	136.53	0.13
20	45	0.6	6	6	88.53	222.55	231.65

## 2.6. Mathematical modeling

After conducting the experiments, the relationships between the dependent and independent variables were calculated using the following equation [26]:

$$Y = \beta_0 + \beta_i X_i + \beta_j X_j + \beta_{ii} X_i^2 + \beta_{jj} X_j^2 + \beta_{ij} X_i X_j + \dots \quad (2)$$

where  $Y$ ,  $i$ ,  $j$ ,  $\beta$ , and  $X$  represent the process response, linear coefficient, quadratic coefficient, regression coefficient, and coded independent variables, respectively. Model terms are accepted or rejected based on the probability of error ( $P$ ) value with 95% confidence level. The results obtained from CCD were entirely examined by means of analysis of variance (ANOVA) using the Design-Expert software. Three-dimensional (3D) plots and their respective contour plots were obtained based on the effects of the levels of the two factors, while other factors can be changed by default. Therefore, the results of the CCD can be presented in 3D presentations with contours. This will help to study the simultaneous interaction of the variables on the responses.

## 3. Results and discussion

### 3.1. Adsorbent characterization

The functionalities of the prepared AC were examined using the FTIR spectra (Fig. 1). The region between 3,200 and 3,600  $\text{cm}^{-1}$  is related to the hydroxyl ( $-\text{OH}$ ) groups, and the two signals at 2,900  $\text{cm}^{-1}$  are assigned to the C–H stretch. Similarly, the presence of  $\text{C}\equiv\text{C}$  structure shows a broad band between 2,200 and 2,400  $\text{cm}^{-1}$ . The strong peak around 1,500  $\text{cm}^{-1}$  has probably resulted from the carboxyl group stretching vibrations. Another important broad peak was detected between 1,000 and 12,000  $\text{cm}^{-1}$ , which is associated to the C–O stretching vibrations.

The scanning electron microscope was used to analyze the surface morphology of AC obtained from India shrub wood. The SEM image (Fig. 2) shows that the prepared AC contained a rough surface with regular tunnel-like structure. In addition, many tiny pores were observed on the surface of the tunnel-like structure. These structures resulted from the remains of dried cell wall would provide a comparatively large surface area.

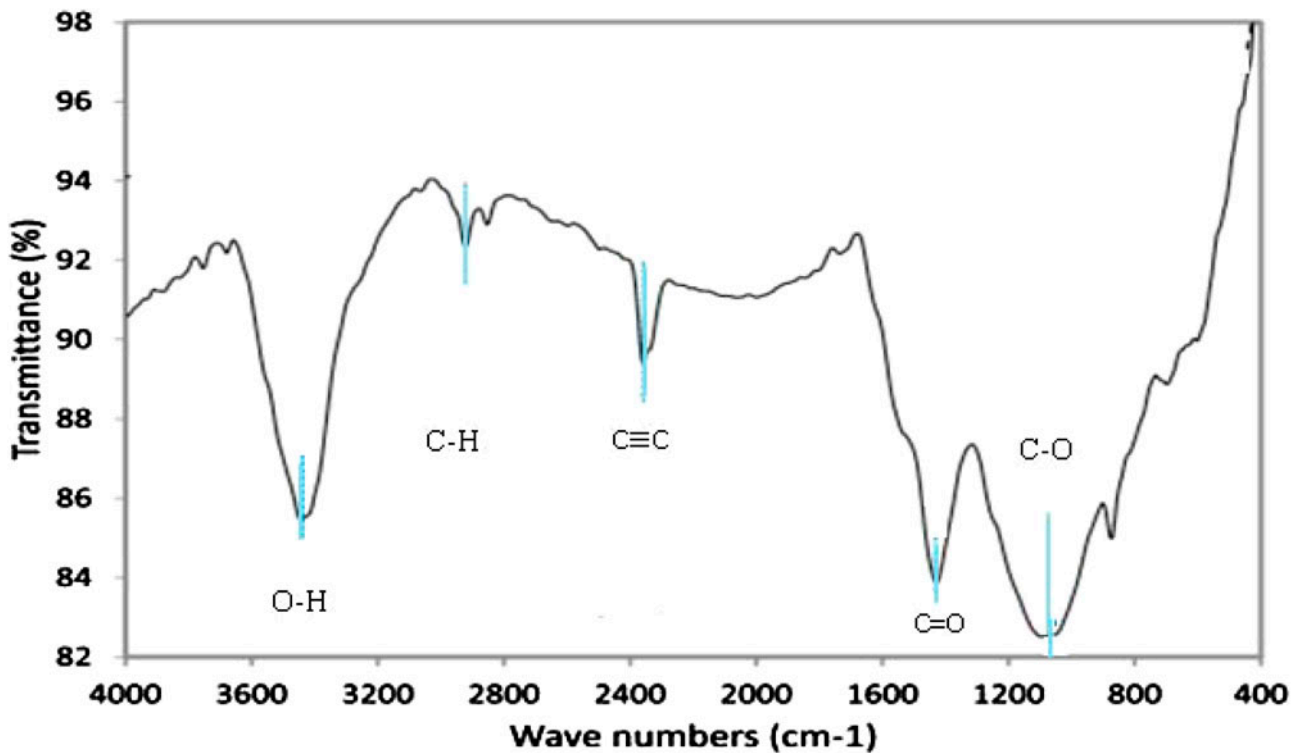


Fig. 1. The FTIR spectrum of India shrub wood powder.

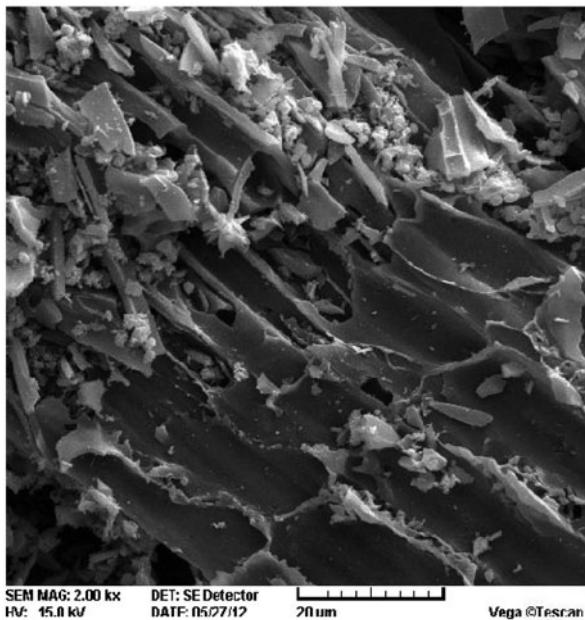


Fig. 2. SEM micrograph of prepared activated carbon.

The BET surface area was determined from adsorption isotherms using a surface area analyzer.

The BET surface area results (Table 1) give a reading of  $1,024 \text{ m}^2/\text{g}$  and a total pore volume of  $0.572 \text{ cm}^3/\text{g}$ . Based on these results, the prepared AC shows high values of the BET surface area and pore volume. According to the International Union of Pure and Applied Chemistry (IUPAC), pores are classified as micropores (<2 nm diameter), mesopores (2–50 nm diameter), and macropores (>50 nm diameter) (IUPAC, 1972). The average pore diameter was found to be 2.23 nm showing that the prepared AC was in the mesopores region.

### 3.2. Model fitting and statistical analysis

The design matrix, in terms of coded factors and experimental results of the adsorption capacity is presented in Table 3. Then, the obtained results were subjected to RSM to evaluate the relationships between the contact time (*A*), adsorbent dosage (*B*), and pH (*C*). The predicted values obtained from model fitting technique and using the Design-Expert software were seen to be sufficiently correlated to the observed values (Table 3). The predicted response values slightly deviated from the experimental data. Multiple regression coefficients of a second-order polynomial model

describing the adsorption capacity are summarized in Table 4. In order to determine the coefficients' significance and suitability of the proposed model, the ANOVA technique was employed. The significance or insignificance of each coefficient was determined using the  $P$ -value. The  $P$ -values lower than 0.05 indicated that the coefficient of a model term is significant. The resulting ANOVA is listed in Table 4 for each of the model terms. Based on the  $P$ -values, the first-order effects of all variables ( $A$ ,  $B$ , and  $C$ ), two-level interaction of  $B$  with  $A$  and  $C$  ( $AB$  and  $BC$ ), and second order of  $A$  are significant model terms. Other model terms are not significant (with a probability value larger than 0.05). These insignificant model terms ( $B^2$ ,  $C^2$ , and  $AC$ ) were eliminated in order to simplify the model.

The ANOVA was also employed to examine the significance of the model fit under an extensive range of operating conditions. The results are depicted in Table 5 (numerically) and Fig. 3 (graphically). The ANOVA results revealed that the quadratic model was significant at the 5% confidence level, respectively, for the adsorption capacity since  $P$  values were less than 0.05. Fisher  $F$ -test value explains the distribution of the actual data around the fitted model. According to the calculated  $F$ -test value (427.51), along with a very low probability value ( $p$  model < 0.0001), it can be concluded that this model is highly significant.

The fitting of models to the empirical data was tested by calculating the determination coefficient ( $R^2$ ). The high value of  $R^2$  (0.995) indicates the capability of the developed model, to satisfactorily describe the system behavior within the investigated range of operating parameters.

Adequate precision (AP) compares the range of the predicted values at the design points to the average prediction errors. Ratios greater than four, indicate an adequate model discrimination and can be used to

navigate the design space defined by the CCD [27]. In this study, the ratio of AP value was found to be 69.64, which is greater than four and can be considered a satisfactory result.

Other important information about fitting, reliability, adequacy, and the correlation between the observed and predicted data of the model performance can be obtained in the diagnostic plots (Fig. 3(a–c)). These figures sufficiently depict any deficiency of the model fitting to the experimental data. Fig. 3(a) displays the normal probability of the response to confirm whether the standard deviations between the actual and the predicted response values follow a normal distribution [28]. Points and points' clusters in the Fig. 3(a) indicated that experimental values are distributed relatively near to the straight line, and satisfactorily shows the correlation between these values. Therefore, there are no serious violations in the hypothesis that errors are normally distributed and are independent of each other [29]. The prediction of adsorption capacity Eq. (3) was compared with the experimental values given in Table 3 and shown in Fig. 3(b). It can be seen from Fig. 3(b) that the model equation prediction is statistically a satisfactory match with the experimental values. Therefore, this model can be used to navigate the design space. In fact, Fig. 3(b) depicts the relationships between the values of  $R^2$  and adjusted  $R^2$ . The  $R^2$  value of 0.995 is in reasonable agreement with the adjusted  $R^2$  values of 0.993, which shows a very good agreement between the predicted and actual data.

The plots of residual against predicted responses (Fig. 3(c)) check the assumption of constant variance. It can be seen that all points of experimental runs are randomly distributed, and that all values lie within the range between  $-3$  and  $3$ . These findings indicated that the model proposed by RSM is satisfactory, and that the constant variance assumptions were confirmed.

Table 4

Estimated regression coefficients and corresponding to ANOVA results from the data of CCD experiments before elimination of insignificant model terms

Model variables	$A$	$B$	$C$	$A^2$	$B^2$	$C^2$	$AB$	$AC$	$BC$
Coefficient estimate	20.46	-131.59	13.29	-7.37	25.92	28.37	-16.91	-3.88	11.02
Standard error	2.62	2.62	2.62	17.70	17.70	3.78	2.70	2.70	2.70
Sum of squares (SS)	3,557.1	1.47*10 <sup>5</sup>	1501.8	10.13	125.4	9,717.8	2,286.6	120.2	971.3
$F$ -value	60.85	2,518.05	25.69	0.17	2.15	2.57	39.12	2.1	16.62
Prob > $F$	< 0.0001	< 0.0001	0.0005	0.686	0.174	< 0.0001	< 0.0001	0.1821	0.009
Significant or insignificant model terms	Sig.	Sig.	Sig.-	Not sig	Not sig.	Sig.	Sig.-	Not sig.	Sig.

Table 5  
ANOVA for fit of  $q_e$  (mg/g) from CCD after elimination of insignificant model terms

Model	Type of model	Significant model terms	F value	Prob > F	SD	R <sup>2</sup>	Adj. R <sup>2</sup>	Pred. R <sup>2</sup>	CV	Adeq. precision	PRESS	Probability for lack of fit
$q$ (mg/g)	Quadratic model	A, B, C, C <sup>2</sup> , AB, BC	427.51	< 0.0001	8.03	0.995	0.993	0.981	3.19	69.645	3157.9	0.058

Notes: R<sup>2</sup>: Determination coefficient, Adj. R<sup>2</sup>: Adjusted R<sup>2</sup>, Adeq. precision: Adequate precision, SD: Standard deviation, and PRESS: Predicted residual error sum of squares.

### 3.3. Interactive effect of the variables on the adsorption capacity

RSM is applied to build-up mathematical relationships between the process variables and the response. According to the results obtained from ANOVA (Table 5), the response surface model, which was constructed in this study for predicting equilibrium adsorption capacity was considered reasonable. The final regression model, in terms of coded factors determined by the Design-Expert software for adsorption capacity is expressed by the following equation:

$$q, \text{ mg/g} = + 231.65 + 20.46 A - 131.59 B + 13.29 C + 46.41 C^2 - 16.91A B - 11.02 BC \quad (3)$$

The relationship between the response and variables was visualized by the three-dimensional surface plots, in order to see the influence of the parameters. Fig. 4(a) shows a three-dimensional contour plot of the model for the variation in the adsorption capacity as a function of the adsorbent dosage and contact time at a constant value of pH (10). The adsorption capacity and percent removal of MB onto the adsorbent drastically increase during the initial adsorption stage (first 5 min), and then continue to increase at a relatively slow speed with a contact time until a state of equilibrium is obtained after 120 min. This phenomenon is related to the fact that a large number of vacant surface sites are available for the adsorption at the initial stage, and after a lapse of time, the remaining vacant surface sites are difficult to be occupied due to the repulsive forces between the solute molecules on the solid and bulk phases. In Fig. 4(a), with an increase in the dose of sorbent, the uptake capacity of MB per unit mass of sorbent ( $q$ , mg/g) decreased while the removal percentage of dye increased. Increasing the sorbent dosage can be attributed to the increased sorbent surface area and the availability of more adsorption sites [20]. But the values of uptake capacity ( $q_e$ ) were decreased with an increase in the sorbent

dosage. The primary factor explaining these characteristics is that the adsorption sites remain unsaturated during the adsorption reaction, whereas the number of sites available for the adsorption site increases with an increase in the adsorbent dose [30].

The effect of the initial pH of the dye solution on the amount of dye adsorbed was studied by varying the initial pH. The results are shown in Fig. 4(b). As shown in this figure, the dye uptake was found to increase with an increase in pH. It was due to the fact that the pH solution can affect the surface charge of the adsorbent, the degree of ionization of the different pollutants, the dissociation of functional groups on the active sites of the adsorbent as well as the structure of the dye molecule.

The surface charge assessed by the point of zero charge ( $\text{pH}_{\text{PZC}}$ ) is defined as the point where the zeta potential is zero. When  $\text{pH} < \text{pH}_{\text{PZC}}$ , the surface charge is positive, and when  $\text{pH} > \text{pH}_{\text{PZC}}$ , the surface charge is negative. In this case, the  $\text{pH}_{\text{PZC}}$  of the adsorbent was about 6.5. When the solution pH is below  $\text{pH}_{\text{PZC}}$ , the adsorbent acquires a positive surface charge. The competitive effects of H<sup>+</sup> ions and the electrostatic repulsion between the cationic dye molecules and the positively charged active adsorption sites on the adsorbent would result in a decrease in the adsorption capacity of dye. In contrast, the surface of the AC may get negatively charged at a solution pH higher than  $\text{pH}_{\text{PZC}}$  [17]. Accordingly, the electrostatic attraction occurs between the negatively charged active adsorption sites and cationic dye molecule, which benefits the adsorption of dye. Increasing pH from 2 to 10 illustrates an enhancement of the adsorption uptake of MB (increased from 349 to 397 mg/g and from 421 to 472 mg/g, respectively, for contact time of 5 and 85 min), primarily due to the electrostatic interaction between the cationic dye molecules and negatively charges surface. In the similar work, the effect of solution pH on the removal of Remazol-Turquoise Blue G-133 from aqueous solution using modified waste newspaper fiber (MWNF) was studied by Zhang et al. [31]. In this study, the maximum

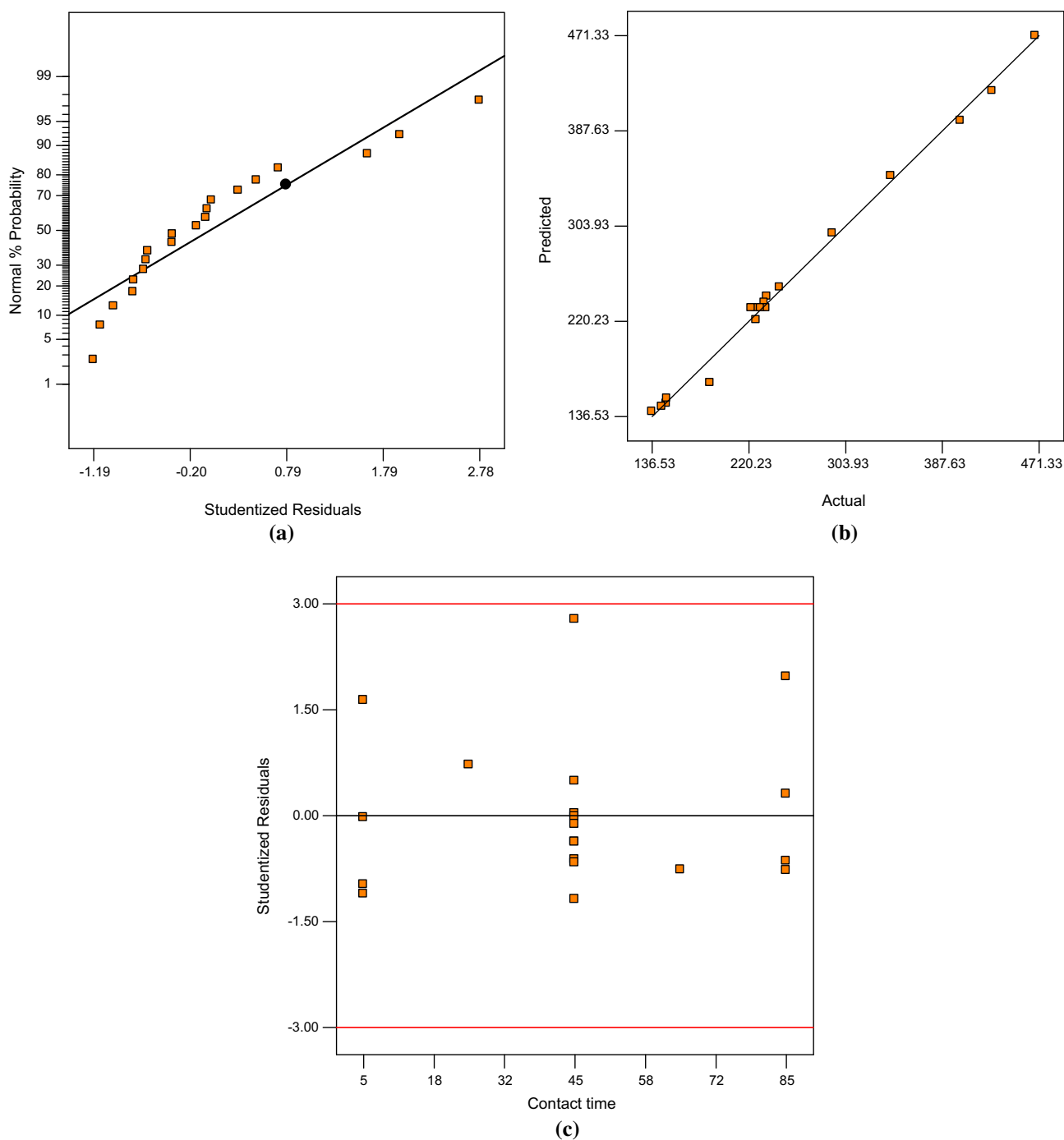


Fig. 3. (a) Normal probability plot of residual, (b) Plot of residual vs. predicted response, and (c) Predicted vs. actual values plot for adsorption capacity of activated carbon produced from India shrub wood.

adsorption capacity of  $260 \text{ mg g}^{-1}$  obtained under pH 2. Under strong acid conditions, the  $\text{SO}_3\text{H}$  group reacts with a quaternary ammonium group to form cell  $\text{R-N}^+(\text{C}_2\text{H}_5)_3\text{SO}_3^-$ . As the pH increases, the  $\text{SO}_3\text{H}$

group is reduced, resulting in the decrease of interaction between the dye molecules and MWNF. Similar adsorption behavior with variation in solution pH has been reported [32].

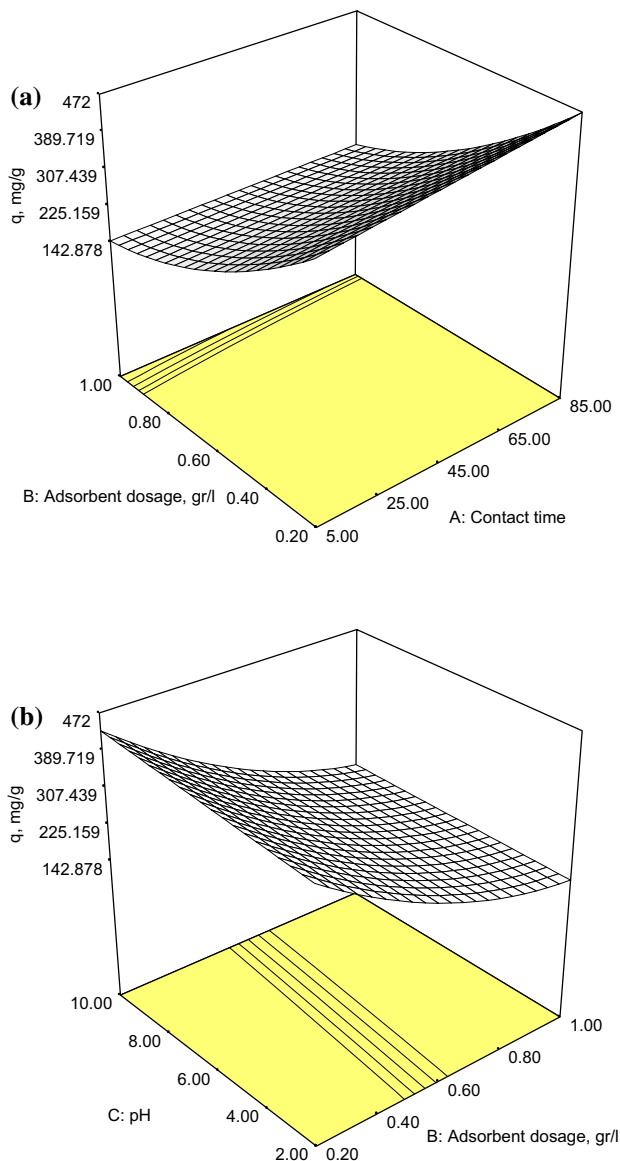


Fig. 4. Response surface plots for MB removal efficiency with respect to (a) adsorbent dosage and contact time (b) pH and adsorbent dosage.

### 3.4. Equilibrium study

Adsorption isotherm describes the interaction between the adsorbate and the carbonaceous adsorbent, and thus is critical for the optimization of the adsorption mechanism pathways. In this study, in order to optimize the design of an adsorption, three adsorption isotherm models, namely Langmuir, Freundlich, and Dubinin–Radushkevich (D–R) models in their linear forms, were used to fit the adsorption experimental data. The applicability of the isotherm equations was compared by judging the correlation

coefficients,  $R^2$ . The Langmuir and Freundlich isotherms are known as two-parameter models, which provide information on the adsorption capacity and constants related to the activation energy.

The Langmuir model states that the adsorption is a process which occurs in a homogeneous surface. The Langmuir isotherm model is suitable for the monolayer adsorption onto a surface with a limited number of similar sites, in which the equation can be written as follows:

$$q_e = \frac{q_0 b C_e}{1 + b C_e} \quad (4)$$

where  $C_e$  is the equilibrium concentration of the adsorbate in the liquid phase (mg/L),  $q_e$  is the concentration of the adsorbate adsorbed at equilibrium (mg/g), and  $q_0$  and  $b$  are the Langmuir constants corresponding to the capacity and energy of adsorption, respectively.

A linear form of Langmuir adsorption isotherm can be obtained by rearranging Eq. (4)

$$\frac{C_e}{q_e} = \frac{1}{q_0 b} + \frac{C_e}{q_0} \quad (5)$$

The linear plots of Langmuir adsorption isotherm ( $C_e/q_e$  vs.  $C_e$ ) in different temperatures were drawn in the Fig. 5(a). All parameters of this adsorption isotherm model and the determined coefficients ( $R^2$ ) are also listed in Table 6 using linear regressive analysis. Compared with values of  $R^2$  listed in Table 6, it was seen that there were higher values of  $R^2$  and adsorption capacity of Langmuir model at 50 and 60°C, respectively. Maximum adsorption capacity was found as 257.73 mg g<sup>-1</sup> at 60°C. It increases with increase in temperature, suggesting endothermic adsorption process. The  $R^2$  values (>0.99) suggest that the Langmuir isotherm provides a good fit to the isotherm data. The values of  $q_0$  increase with a temperature increase, thereby confirming that the process is endothermic. A similar observation was reported for the adsorption of MB on fly ash [33], pomelo (*Citrus grandis*) [14], silk worm [34], cedar sawdust, and crushed brick [35].

$R_L$  as a dimensionless constant separation factor has been defined to evaluate the validity of the Langmuir-type adsorption process [36,37]:

$$R_L = \frac{1}{1 + b C_0} \quad (6)$$

where  $C_0$  is the initial concentration of the adsorbate and  $b$  is the Langmuir isotherm constant. However,

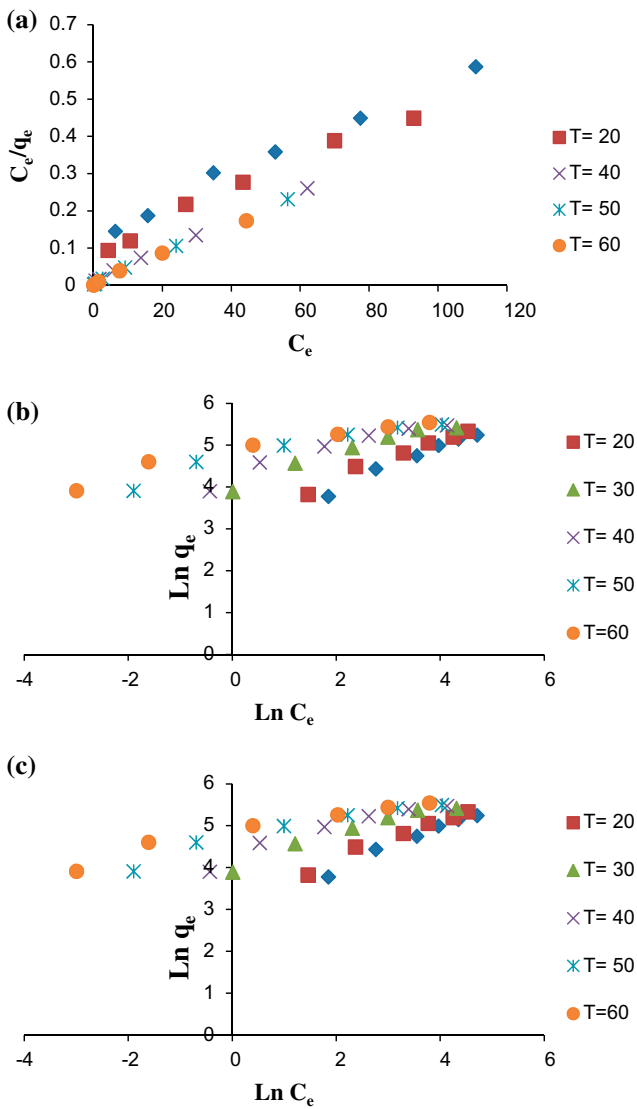


Fig. 5. Isotherm plots for the adsorption of MB onto adsorbent (a) Langmuir isotherm, (b) Freundlich isotherm, and (c) Dubinin–Radushkevich isotherms at different temperatures.

for practical purposes, the following  $R_L$  values can be used to assess the degree of adsorption [38].

- $R_L = 0$ : irreversible
- $0 < R_L < 1$ : favorable
- $R_L > 1$ : unfavorable

For the value range of different temperatures (10–60°C), the  $R_L$  values decreased from 0.08 to 0.004, indicating that the adsorption of MB onto adsorbent is favorable.

The Freundlich isotherm is an empirical equation employed to describe heterogeneous systems. A linear

form of the Freundlich isotherm will yield the constants  $K_f$  and  $n$  is given by:

$$\ln q_e = \ln K_f + \frac{1}{n} \ln C_e \tag{7}$$

where  $K_f$  and  $n$  are Freundlich constants that can be attributed to the adsorption capacity and adsorption intensity, respectively, and that it can be calculated from the intercept and slope of the plot of  $\ln q_e$  vs.  $\ln C_e$ . The magnitude of the exponent  $1/n$  gives an indication of the favorability of the adsorption. Values of  $n > 1$  represent the favorable adsorption condition [39]. This isotherm is appropriate for the adsorption on a heterogeneous surface and is not limited to the monolayer formation. The results obtained from the slope and the intercept in Fig. 5(b) shows that the Freundlich isotherm model showed good fit to the experimental equilibrium adsorption data ( $R^2 > 0.92$ ). The values of  $K_f$  and  $1/n$  are listed in Table 6. In general, with an increase in the  $K_f$  value, the adsorption capacity of the adsorbent increases. The values of  $K_f$  and  $n$  were found to be 119.94 (mg/g (L/mg)<sup>1/n</sup>) and 6, respectively (Fig. 5(b) and Table 6). The value of Freundlich exponent  $n$  (6) is the range of  $n > 1$ , indicating a favorable adsorption.

The adsorption equilibrium data were also tested for another isotherm model, Dubinin–Radushkevich (D–R). The D–R equation has the following linear form [40]:

$$\ln q_e = \ln V_m - K \varepsilon^2 \tag{8}$$

where  $q_e$  is the MB amount that is removed per unit adsorbate mass (mg/g),  $V_m$  is the D–R sorption capacity (mg/g),  $K$  is the constant related to the adsorption energy (mol<sup>2</sup> kJ<sup>2</sup>), and  $\varepsilon$  is the Polanyi potential.

According to Eq. (8), the Polanyi potential ( $\varepsilon$ ) can be given as:

$$\varepsilon = RT \ln (1 + 1/C_e) \tag{9}$$

where  $R$  is the gas constant (kJ/K mol) and  $T$  is the temperature (K). The main energy of the adsorption  $E$  (kJ/mol) is calculated using the following formula:

$$E = (-2K)^{-0.5} \tag{10}$$

where  $E$  gives information about the physical and chemical features of adsorption.

A plot of  $\ln q_e$  against  $\varepsilon^2$  is given in Fig. 5(c).

D–R isotherm parameters were calculated from the slope of curve in Fig. 5(c) and mean energy was found

Table 6

Langmuir, Freundlich, and Dubinin–Radushkevich constants and correlation coefficients for the adsorption of MB in different temperatures at MB concentration of 50–300 mg/L

Temp (K)	Langmuir				Freundlich			Dubinin–Radushkevich (D–R)			
	$q_0$ (mg MB/g)	$b$ (L/mg)	$R_L$	$R^2$	$K$ (L/g)	$n$	$R^2$	$k$	$E$	$V_m$	$R^2$
10	219.29	0.034	0.08	0.992	18.58	1.96	0.948	4.9	0.35	152.93	0.83
20	227.79	0.049	0.06	0.986	25.69	2.13	0.935	4.97	0.5	155.86	0.838
30	238.09	0.21	0.02	0.997	56.37	2.78	0.932	0.44	1.73	173.29	0.816
40	241.31	0.29	0.01	0.998	70.67	3.01	0.95	0.238	2.42	185.86	0.872
50	246.91	0.61	0.005	0.998	100.58	3.92	0.977	0.047	5.4	191.904	0.889
60	257.73	0.8	0.004	0.996	119.94	4.46	0.98	0.02	8.4	198.74	0.9

to be in the range of 0.35–8.4 kJ mol<sup>-1</sup>. Low value of mean energy of the adsorption demonstrated that the adsorption process showed physical characteristics [41]. According to the evaluated models, D–R models isotherm does not explain this adsorption process whereas Langmuir and Freundlich do.

### 3.5. Adsorption kinetics

The adsorption kinetics is an important part of every adsorption study because it represents critical parameters (e.g. presenting the adsorption rate,

predicting the  $q_e$  values, etc.) in designing an industrial adsorption column.

In order to study the controlling mechanisms of the adsorption process, pseudo-first-order (Eq. (11)), pseudo-second-order (Eq. (12)), intraparticle diffusion (Eq. (13)), and Elovich (Eq. (14)) equation models were employed to analyze the experimental kinetic data.

- Pseudo-first-order model:

$$\ln(q_e - q_t) = \ln q_e - \frac{k_1}{2.303} t \quad (11)$$

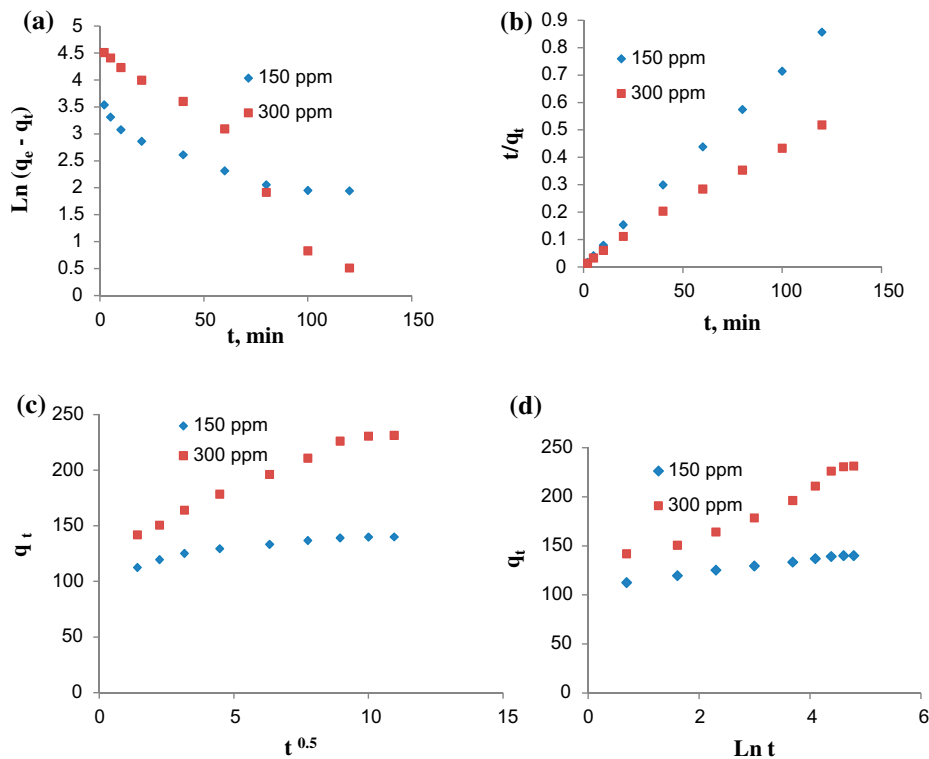


Fig. 6. Plots of pseudo-first-order (a), pseudo-second-order (b), Intraparticle diffusion (c), and Elovich kinetic model for the MB concentration of 150 and 300 mg/L.

Table 7  
Kinetic model parameters for the adsorption MB at different concentration on pumice powder

Kinetic model parameters	Kinetic parameters	MB concentration (mg/L)	
		150	300
Pseudo-first-order	$K_1$	0.03	0.08
	$R^2$	0.91	0.97
Pseudo-second-order	$K_2$	0.005	0.0008
	$R^2$	0.999	0.997
Intraparticle diffusion model	$k_p$	9.91	2.68
	$R^2$	0.98	0.91
Elovich model	$\alpha$	115.7	844.2
	$\beta$	0.84	0.53
	$R^2$	0.94	0.88

- Pseudo-second-order model:

$$\frac{t}{q_t} = \frac{t}{q_e} + \frac{1}{k_2 q_e^2} \quad (12)$$

- Intraparticle diffusion model:

$$q_t = k_p t^{0.5} \quad (13)$$

- Elovich model:

$$q_t = \left(\frac{1}{\beta}\right) \ln(\alpha\beta) + \left(\frac{1}{\beta}\right) \ln t \quad (14)$$

where  $q_e$  (mg/g) and  $q_t$  (mg/g) are the amounts of MB adsorbed by the adsorbate at equilibrium and at different time intervals, respectively.  $k_1$  (1/min) and  $k_2$  (g/mg min) are the pseudo-first-order and pseudo-second-order rate constants,  $k_p$  is the intraparticle diffusion rate constant (mg/g min<sup>0.5</sup>), and  $\alpha$  (mg/g min) and  $\beta$  (g/mg) are Elovich constants. The linear plots [ $\log(q_t - q_e)$  vs.  $t$ ], [ $t/q_t$  vs.  $t$ ], [ $q_t$  vs.  $t^{0.5}$ ], and [ $q_t$  vs.  $\ln t$ ] allowed the validity of the different models to be checked. Fig. 6 shows the linearized form of the different kinetic models. The kinetic parameters calculated from Eqs. (11)–(14) for the adsorption of MB at two different concentrations of dye (150 and 300 mg/L) on the adsorbent are given in Table 7. According to Table 3, the regression correlation coefficients ( $R^2$ ) for all models were greater than 0.9 in different concentrations because the highest values were observed for the pseudo-second kinetic model ( $R^2 > 99$ ). This result indicated that the adsorption of MB onto this

adsorbent follows the pseudo-second-order kinetic model very well, which is similar to previous studies in the literature [42,43]. This suggests that the rate of the adsorption process is preferably controlled by the chemisorption, which is also reported by Kaur et al. [44], who studied the MB adsorption onto KOH/CO<sub>2</sub>-AC from coconut. Table 7 indicates that the  $q_e$  values increased with an increase in the initial dye concentrations, but the rate constants ( $k_1$  values) decreased with an increase in  $C_0$ . At higher MB concentrations, the competition for the surface sorption sites will be high, which will consequently lead to a comparatively low-rate constant [45].

### 3.6. Thermodynamic study

In order to calculate the thermodynamic parameters, such as Gibbs free energy ( $\Delta G^\circ$ ), enthalpy ( $\Delta H^\circ$ ), and entropy ( $\Delta S^\circ$ ), adsorption experiments were carried out at different temperatures (10, 20, 30, 40, 50, and 60°C). An increase in the temperature from 10 to 60°C increased the adsorption capacity from 219.29 to

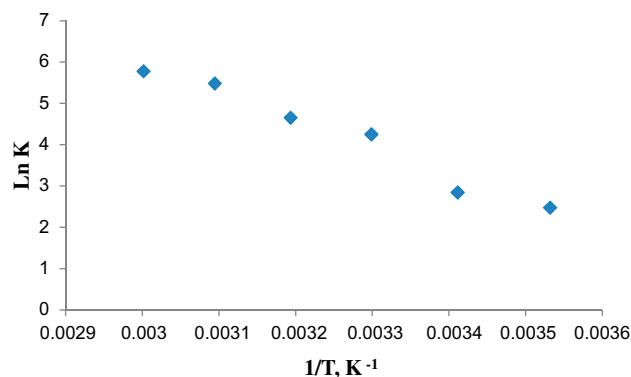


Fig. 7. Vant's Hoff plot for the determination of thermodynamic parameters.

Table 8

Adsorption capacities for activated carbons derived from agricultural and industrial wastes

Adsorbents	Adsorption capacity (mg/g)	Sources
India shrub wood	257.73	This study
M-MWCNTs	48.06	[47]
Jute fiber carbon	225.6	[48]
Groundnut shell activated carbon	164.9	[49]
Activated sludge biomass	256.41	[50]
Diatomite	156.6	[51]
Bituminous coal	176	[52]
Algae Gelidium	171	[53]
Alga <i>Sargassum muticum</i> seaweed	279.2	[54]

257.73 mg/g. The values of  $\Delta H^\circ$ ,  $\Delta G^\circ$ , and  $\Delta S^\circ$  were computed according to the following equations:

$$\ln K_L = \frac{\Delta S^\circ}{R} - \frac{\Delta H^\circ}{RT} \quad (15)$$

$$\Delta G^\circ = \Delta H^\circ - T \Delta S^\circ \quad (16)$$

where  $R$  is the gas constant,  $K_L$  is the Langmuir constant, and  $T$  is the temperature.

The values of  $\Delta H^\circ$  and  $\Delta S^\circ$  were calculated from the slope and intercept of the linear variation of  $\ln K$  and  $1/T$  and found to be  $56.14 \text{ kJ mol}^{-1}$  and  $0.218 \text{ kJ mol}^{-1} \text{ K}^{-1}$ , respectively (Fig. 7).

The negative values of  $\Delta G^\circ$  ( $-5.45$ ,  $-7.63$ ,  $-9.8$ ,  $-11.98$ ,  $-14.15$ , and  $-16.3$ ) indicate the spontaneous nature of the adsorption of MB at 10, 20, 30, 40, 50, and  $60^\circ\text{C}$ , and confirm the affinity of the sorbent for the dyes [21]. The positive value of  $\Delta H^\circ$  ( $56.14 \text{ kJ mol}^{-1}$ ) shows the endothermic nature of the adsorption. The positive value of  $\Delta S^\circ$  ( $0.218 \text{ kJ mol}^{-1} \text{ K}^{-1}$ ) suggests the increased randomness at the solid/solution interface during the adsorption of dye on the adsorbate.

Generally, the change of free energy for the physisorption is between 0 and  $-20 \text{ kJ mol}^{-1}$ , the physisorption together with the chemisorption is in the range from  $-20$  to  $-80 \text{ kJ mol}^{-1}$ , and the chemisorption is at a range from  $-80$  to  $-400 \text{ kJ mol}^{-1}$  [46]. The adsorption of MB onto this adsorbent, with the enthalpy of  $56.14 \text{ kJ mol}^{-1}$ , is at the state between physical and chemical adsorption.

Table 8 compares the adsorption capacity of AC obtained in this study with different adsorbents previously employed to remove MB from aqueous solutions. The adsorption capacity of MB onto this adsorbent is higher than that of many other previously reported adsorbents [47–54], suggesting that the

prepared AC has great potential application in the removal of dye from aqueous solution.

#### 4. Conclusion

The results obtained from this study, clearly suggest that the AC produced from India shrub wood acts as a well adsorbent for the removal of MB from aqueous solutions. The surface area of the AC was found to be  $1,024 \text{ m}^2/\text{g}$ , which is relatively high compared with the MB high adsorption capacity. The obtained results were modeled using three isotherm models: Langmuir, Freundlich, and Dubinin–Radushkevich. Equilibrium isotherms were well described by the Langmuir equation, giving a maximum adsorption capacity of  $257.73 \text{ mg/g}$  at  $60^\circ\text{C}$ . The adsorption kinetics can be adequately described by the pseudo-second-order model equation. In order to better understand the different stages of the adsorption at varying contact time, pH, and sorbent dosages, RSM was used to optimize MB uptake. According to the thermodynamic study, the adsorption of MB on this adsorbent with the enthalpy of  $56.14 \text{ kJ mol}^{-1}$  is at the state between physical and chemical sorption.

#### Acknowledgments

This letter resulted from Thesis, Major, Environmental Health Engineering of Kermanshah University of Medical Sciences, Kermanshah, Iran.

#### References

- [1] M. Huang, C. Xu, Z. Wu, Y. Huang, J. Lin, J. Wu, Photocatalytic discolorization of methyl orange solution by Pt modified  $\text{TiO}_2$  loaded on natural zeolite, *Dyes Pigm.* 77 (2008) 327–334.
- [2] E.V. Veliev, T. Ozturk, S. Veli, A.G. Fatullayev, Application of diffusion model for adsorption of azo

- reactive dye on pumice, Polish J. Environ. Stud. 15 (2006) 347–353.
- [3] I.M. Banat, P. Nigam, D. Singh, R. Marchant, Microbial decolorization of textile-dye containing effluents: A review, *Bioresour. Technol.* 58 (1996) 217–227.
- [4] T. Robinson, G. McMullan, R. Marchant, P. Nigam, Remediation of dyes in textile effluent: A critical review on current treatment technologies with a proposed alternative, *Bioresour. Technol.* 77 (2001) 247–255.
- [5] J.H. Mo, Y.H. Lee, J. Kim, J.Y. Jeong, J. Jegal, Treatment of dye aqueous solutions using nanofiltration polyamide composite membranes for the dye wastewater reuse, *Dyes Pigm.* 76 (2008) 429–434.
- [6] Y.C. Sharma, Uma, S.N. Singh, Paras, F. Gode, Fly ash for the removal of Mn(II) from aqueous solutions and wastewaters, *Chem. Eng. J.* 132 (2007) 319–323.
- [7] C.H. Weng, Y.C. Sharma, S.H. Chu, Adsorption of Cr (VI) from aqueous solutions by spent activated clay, *J. Hazard. Mater.* 155 (2008) 65–75.
- [8] M. Ahmedna, W.E. Marshall, R.M. Rao, Production of granular activated carbons from select agricultural by-products and evaluation of their physical, chemical and adsorption properties, *Bioresour. Technol.* 71 (2000) 113–123.
- [9] M. Matto, Q. Husain, Decolorization of direct dyes by salt fractionated turnip proteins enhanced in the presence of hydrogen peroxide and redox mediators, *Chemosphere* 69 (2007) 338–345.
- [10] C. Michailof, G.G. Stavropoulos, C. Panayiotou, Enhanced adsorption of phenolic compounds, commonly encountered in olive mill wastewaters, on olive husk derived activated carbons, *Bioresour. Technol.* 99 (2008) 6400–6408.
- [11] S. Senthilkumar, P.R. Varadarajan, K. Porkodi, C.V. Subbhuraam, Adsorption of methylene blue onto jute fiber carbon: Kinetics and equilibrium studies, *J. Colloid Interface Sci.* 284 (2005) 78–82.
- [12] P. Pengthamkeerati, T. Satapanajaru, O. Singchan, Sorption of reactive dye from aqueous solution on biomass fly ash, *J. Hazard. Mater.* 153 (2008) 1149–1156.
- [13] J.V. Nabais, P. Carrott, M.M.L. Ribeiro Carrott, V. Luz, A.L. Ortiz, Influence of preparation conditions in the textural and chemical properties of activated carbons from a novel biomass precursor: The coffee endocarp, *Bioresour. Technol.* 99 (2008) 7224–7231.
- [14] R. Han, D. Ding, Y. Xu, W. Zou, Y. Wang, Y. Li, L. Zou, Use of rice husk for the adsorption of congo red from aqueous solution in column mode, *Bioresour. Technol.* 99 (2008) 2938–2946.
- [15] R.L. Tseng, Physical and chemical properties and adsorption type of activated carbon prepared from plum kernels by NaOH activation, *J. Hazard. Mater.* 147 (2007) 1020–1027.
- [16] S. Sumanjit, R.K. Rani Mahajan, Equilibrium, kinetics and thermodynamic parameters for adsorptive removal of dye Basic Blue 9 by ground nut shells and *Eichhornia*, *Arabian J. Chem.* Available from: <<http://dx.doi.org/10.1016/j.arabjc.2012.03.013>>.
- [17] A.E. Ofomaja, Y.S. Ho, Equilibrium sorption of anionic dye from aqueous solution by palm kernel fibre as sorbent, *Dyes Pigm.* 74 (2007) 60–66.
- [18] B.H. Hameed, A.T.M. Din, A.L. Ahmad, Adsorption of methylene blue onto bamboo-based activated carbon: Kinetics and equilibrium studies, *J. Hazard. Mater.* 141 (2007) 819–825.
- [19] B. Zhao, W. Xiao, Y. Shang, H. Zhu, R. Han, Adsorption of light green anionic dye using cationic surfactant-modified peanut husk in batch mode, *Arabian J. Chem.* Available from: <<http://dx.doi.org/10.1016/j.arabjc.2014.03.010>>.
- [20] S., Sumanjit, R.K. Mahajan, G.V. Kumar, Modification of surface behavior of *Eichhornia crassipes* using surface active agent: An adsorption study, *Ind. Eng. Chem.* Available from: <<http://dx.doi.org/10.1016/j.jiec.2014.02.024>>.
- [21] S. Kaur, S. Rani, R.K. Mahajan, Adsorption of dye crystal violet onto surface-modified *Eichhornia crassipes*, *Desalin. Water Treat.* Available from: <<http://dx.doi.org/10.1080/19443994.2013.841109>>.
- [22] A.L. Cazetta, A.M.M. Vargas, E.M. Nogami, M.H. Kunita, M.R. Guilherme, A.C. Martins, T.L. Silva, J.C.G. Moraes, V.C. Almeida, NaOH-activated carbon of high surface area produced from coconut shell: Kinetics and equilibrium studies from the methylene blue adsorption, *Chem. Eng. J.* 174 (2011) 117–125.
- [23] A.A.L. Zinatizadeh, A.R. Mohamed, A.Z. Abdullah, M.D. Mashitah, M. Hasnain Isa, G.D. Najafpour, Process modeling and analysis of palm oil mill effluent treatment in an up-flow anaerobic sludge fixed film bioreactor using response surface methodology (RSM), *Water Res.* 40 (2006) 3193–3208.
- [24] Y. Mansouri, A. Zinatizadeh, P. Mohammadi, M. Irandoust, A. Akhbari, R. Davoodi, Hydraulic characteristics analysis of an anaerobic rotatory biological contactor (AnRBC) using tracer experiments and response surface methodology (RSM), *Korean J. Chem. Eng.* 29 (2012) 891–902.
- [25] F. Shahrezaei, Y. Mansouri, A.A.L. Zinatizadeh, A. Akhbari, Process modeling and kinetic evaluation of petroleum refinery wastewater treatment in a photocatalytic reactor using TiO<sub>2</sub> nanoparticles, *Powder Technol.* 221 (2012) 203–212.
- [26] A.I. Khuri, J.A. Cornell, *Response Surfaces, Design and Analyses*, second ed., Marcel Dekker Inc., New York, NY, 1996.
- [27] R.L. Mason, R.F. Gunst, J.L. Hess, *Statistical Design and Analysis of Experiments, Eighth Applications to Engineering and Science*, second ed., Wiley, New York, NY, 2003.
- [28] K.-M. Lee, D.F. Gilmore, Formulation and process modeling of biopolymer (polyhydroxyalkanoates: PHAs) production from industrial wastes by novel crossed experimental design, *J. Process Biochem.* 40 (1) (2005) 229–246.
- [29] H. Kusic, N. Koprivanac, A.L. Bozic, Treatment of chlorophenols in water matrix by UV/ferri-oxalate system: Part II. Degradation mechanisms and ecological parameters evaluation, *Desalination* 280 (2011) 208–216.
- [30] F. Ghorbani, H. Younesi, S.M. Ghasempouri, A.A. Zinatizadeh, M. Amini, A. Daneshi, Application of response surface methodology for optimization of cadmium biosorption in an aqueous solution by *Saccharomyces cerevisiae*, *Chem. Eng. J.* 145 (2008) 267–275.
- [31] X. Zhang, J. Tan, X. Wei, L. Wang, Removal of Remazol turquoise Blue G-133 from aqueous solution using modified waste newspaper fiber, *Carbohydr. Polym.* 92 (2013) 1497–1502.

- [32] Y. Qi, J. Li, L. Wang, Removal of Remazol Turquoise Blue G-133 from aqueous medium using functionalized cellulose from recycled newspaper fiber, *Ind. Crops Prod.* 50 (2013) 15–22.
- [33] K.V. Kumar, V. Ramamurthi, S. Sivanesan, Modeling the mechanism involved during the sorption of methylene blue onto fly ash, *J. Colloid Interface Sci.* 284 (2005) 14–21.
- [34] B. Noroozi, G.A. Sorial, H. Bahrami, M. Arami, Equilibrium and kinetic adsorption study of a cationic dye by a natural adsorbent—Silkworm pupa, *J. Hazard. Mater.* 139 (2007) 167–174.
- [35] O. Hamdaoui, Batch study of liquid-phase adsorption of methylene blue using cedar sawdust and crushed brick, *J. Hazard. Mater.* 135 (2006) 264–273.
- [36] G. McKay, The adsorption of dyestuffs from aqueous solution using activated carbon: Analytical solution for batch adsorption based on external mass transfer and, *Chem. Eng. J.* 27 (1983) 187–196.
- [37] T.W. Weber, R.K. Chakravorti, Pore and solid diffusion models for fixed-bed adsorbers, *AIChE J.* 20 (1974) 228–238.
- [38] S. Samatya, N. Kabay, Ü. Yüksel, M. Arda, M. Yüksel, Removal of nitrate from aqueous solution by nitrate selective ion exchange resins, *React. Funct. Polym.* 66 (2006) 1206–1214.
- [39] B.H. Hameed, R.R. Krishni, S.A. Sata, A novel agricultural waste adsorbent for the removal of cationic dye from aqueous solutions, *J. Hazard. Mater.* 162 (2009) 305–311.
- [40] S. Veli, B. Alyüz, Adsorption of copper and zinc from aqueous solutions by using natural clay, *J. Hazard. Mater.* 149 (2007) 226–233.
- [41] Y. Feng, F. Yang, Y. Wang, L. Ma, Y. Wu, P.G. Kerr, L. Yang, Basic dye adsorption onto an agro-based waste material—Sesame hull (*Sesamum indicum L.*), *Biore-sour. Technol.* 102 (2011) 10280–10285.
- [42] D.K. Mahmoud, M.A.M. Salleh, W.A.W.A. Karim, A. Idris, Z.Z. Abidin, Batch adsorption of basic dye using acid treated kenaf fibre char: Equilibrium, kinetic and thermodynamic studies, *Chem. Eng. J.* 181–182 (2012) 449–457.
- [43] I.A.W. Tan, A.L. Ahmad, B.H. Hameed, Adsorption of basic dye on high-surface-area activated carbon prepared from coconut husk: Equilibrium, kinetic and thermodynamic studies, *J. Hazard. Mater.* 154 (2008) 337–346.
- [44] S. Kaur, S. Rani, R.K. Mahajan, Adsorptive removal of dye crystal violet onto low-cost carbon produced from *Eichhornia* plant: kinetic, equilibrium, and thermodynamic studies, *Desalin. Water Treat.* Available from: <<http://dx.doi.org/10.1080/19443994.2013.859104>>.
- [45] S. Nethaji, A. Sivasamy, Adsorptive removal of an acid dye by lignocellulosic waste biomass activated carbon: Equilibrium and kinetic studies, *Chemosphere* 82 (2011) 1367–1372.
- [46] M.J. Jaycock, G.D. Parfitt, *Chemistry of Interfaces*. Ellis Horwood Ltd., Chichester, 1981.
- [47] A. Lunhong, Z. Chunying, L. Fang, W. Yao, L. Ming, M. Lanying, J. Jing, Removal of methylene blue from aqueous solution with magnetite loaded multi-wall carbon nanotube: Kinetic, isotherm and mechanism analysis, *J. Hazard. Mater.* 198 (2011) 282–290.
- [48] S. Senthilkumar, P.R. Varadarajan, K. Porkodi, C.V. Subbhuraam, Adsorption of methylene blue onto jute fiber carbon: Kinetics and equilibrium studies, *J. Colloid Interface Sci.* 284 (2005) 78–82.
- [49] N. Kannan, M.M. Sundaram, Kinetics and mechanism of removal of methylene blue by adsorption on various carbons—A comparative study, *Dyes Pigm.* 51 (2001) 25–40.
- [50] O. Gulnaz, A. Kaya, F. Matyar, B. Arikian, Sorption of basic dyes from aqueous solution by activated sludge, *J. Hazard. Mater.* 108 (2004) 183–188.
- [51] M.A. Al-Ghouti, M.A.M. Khraisheh, S.J. Allen, M.N. Ahmad, The removal of dyes from textile wastewater: A study of the physical characteristics and adsorption mechanisms of diatomaceous earth, *J. Environ. Manage.* 69 (2003) 229–238.
- [52] F. Banat, S. Al-Asheh, R. Al-Ahmad, F. Bni-Khalid, Bench-scale and packed bed sorption of methylene blue using treated olive pomace and charcoal, *Biore-sour. Technol.* 98 (2007) 3017–3025.
- [53] V.J.P. Vilar, C.M.S. Botelho, R.A.R. Boaventura, Methylene blue adsorption by algal biomass based materials: Biosorbents characterization and process behaviour, *J. Hazard. Mater.* 147 (2007) 120–132.
- [54] E. Rubin, P. Rodriguez, R. Herrero, J. Cremades, I. Barbara, M.E. Sastre deVicente, Removal of methylene blue from aqueous solutions using as biosorbent *Sargassum muticum*: An invasive macroalga in Europe, *J. Chem. Technol. Biotechnol.* 80 (2005) 291–298.